

# ISOTHERMAL SOLIDIFICATION DURING TRANSIENT LIQUID-PHASE BONDING OF GTD-111/Ni-Si-B/GTD-111

## IZOTERMNO STRJEVANJE MED SPAJANJEM GTD-111/Ni-Si-B/GTD-111 S PREHODNO TEKOČO FAZO

Majid Pouranvari

Young Researchers and Elite Club, Dezful Branch, Islamic Azad University, Dezful, Iran  
mpouranvari@yahoo.com

Prejem rokopisa – received: 2013-04-23; sprejem za objavo – accepted for publication: 2013-05-20

A prediction of the required time to ensure the completion of isothermal solidification ( $t_{IS}$ ) can serve as a first step toward the optimization of a transient-liquid-phase (TLP) process to achieve a eutectic-free joint. The objective of this study is to estimate the required bonding time to obtain an intermetallic-free joint centerline during the TLP bonding of a cast GTD-111 nickel-based superalloy using a Ni-4.5Si-3.2B (mass fractions, w%) amorphous interlayer. Considering the solidification behaviour of the residual liquid,  $t_{IS}$  could be predicted by a mathematical solution of the time-dependent diffusion equation based on Fick's second law.

Keywords: transient-liquid-phase bonding, isothermal solidification, superalloy, GTD-111

Napovedovanje potrebnega časa za zagotavljanje poteka izotermnega strjevanja ( $t_{IS}$ ) se lahko uporablja kot prvi približek za optimizacijo postopka spajanja s prehodno tekočo fazo (TLP) za doseganje spojev brez evtektika. Namen te študije je ugotoviti potreben čas spajanja za doseganje srednje linije spoja brez intermetalnih faz med TLP-spajanjem nikljeve GTD-111 superzlitine s strjevalno strukturo z uporabo Ni-4,5Si-3,2B (masni deleži, w%) amorfnе vmesne plasti. Z upoštevanjem vedenja preostale taline pri strjevanju je mogoče  $t_{IS}$  napovedati z matematično rešitvijo časovne odvisnosti difuzijske enačbe, ki temelji na drugem Fickovem zakonu.

Ključne besede: spajanje s prehodno tekočo fazo, izotermno strjevanje, superzlitina, GTD-111

## 1 INTRODUCTION

Nickel-based superalloys are used extensively in modern industry due to their excellent high-temperature tensile strength, stress rupture and creep properties, fatigue strength, oxidation and corrosion resistance, and microstructural stability at elevated temperature.<sup>1-3</sup>

Transient-liquid-phase (TLP) bonding is considered as an interesting repairing/joining process for nickel-based superalloys due to its ability to produce near-ideal joints.<sup>4-12</sup> The TLP process nominally involves three stages: (i) when heated, the braze melts and begins to dissolve the substrate; (ii) the liquid composition reaches the liquidus and isothermal precipitation of the equilibrium solid begins; (iii) the liquid is eliminated by diffusion of the melting-point modifiers into the substrate (i.e., isothermal solidification).<sup>13,14</sup>

The typical microstructure of a TLP bonded joint of a nickel-based precipitation-hardened superalloy such as GTD-111 using a boron-containing interlayer, consists of three distinct microstructural zones, before completion of the isothermal solidification (**Figure 1**):<sup>6-9</sup>

- the Athermally Solidified Zone (ASZ), which usually consists of an intermetallic formed during a eutectic reaction. This zone is formed due to there being insufficient time for completion of the isothermal solidification. Cooling is the main driving force for athermal solidification (i.e., non-isothermal solidification).

- the Isothermally Solidified Zone (ISZ), which usually consists of a solid-solution phase. A compositional change induced by interdiffusion between the substrate and the interlayer during holding at a constant bonding temperature is the driving force for the isothermal solidification. As a result of the absence of solute rejection at the solid/liquid interface during isothermal solidification under equilibrium, the formation of a second phase is basically prevented.<sup>7,8</sup>
- the Diffusion Affected Zone (DAZ), which consists of boride precipitates due to boron diffusion into the base metal (BM) during the TLP bonding.

For the commercial application of TLP bonding, the appropriate holding time required for complete isothermal solidification ( $t_{IS}$ ) should be determined to obtain

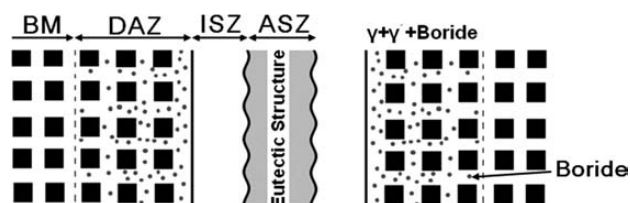


**Figure 1:** Schematic representation of various microstructural zones in a TLP-bonded  $\gamma'$ -strengthened nickel-based superalloy before isothermal solidification completion

**Slika 1:** Shematski prikaz mikrostrukture v različnih območjih v TLP spajani superzlitini na osnovi niklja z  $\gamma'$ -delci za utrjevanje pred koncem izotermnega strjevanja

the proper bond microstructure. When the holding time is lower than  $t_{IS}$ , athermal solidification of the residual liquid phase may lead to intermetallic formation, which in turn degrades the mechanical strength, service temperature and corrosion resistance of the bonds compared to the base metal.<sup>4-10</sup>

In this paper a diffusion model based on a migrating interface is used to predict the isothermal solidification completion time during the TLP bonding of a GTD-111 nickel-based superalloy and the predicted value was compared with experimental data.

## 2 EXPERIMENTAL PROCEDURE

The GTD-111 superalloy, as the base metal, was used in the standard heat-treatment condition in this investigation. The chemical composition of the GTD-111 was Ni-13.5 Cr-9.5 Co-4.75 Ti-3.3 Al-3.8 W-1.53 Mo-2.7 Ta-0.23 Fe-0.09 C. A commercial Ni-4.5Si-3.2B alloy (MBF30), in the form of amorphous foil with 25.4  $\mu\text{m}$  thickness, was used as the interlayer. Coupons of 10 mm  $\times$  5 mm  $\times$  5 mm were sectioned using an electro-discharge machine. To remove the oxide layer, contact surfaces were ground using 600-grade SiC paper and then cleaned ultrasonically in an acetone bath. The

interlayer was then inserted between two base metal coupons. A stainless-steel fixture was used to fix the coupons in order to hold the sandwich assembly and reduce the metal flow during the TLP operation. The liquidus and solidus temperatures of the interlayer are 1054  $^{\circ}\text{C}$  and 894  $^{\circ}\text{C}$ , respectively.<sup>15</sup> The bonding was carried out at 1100  $^{\circ}\text{C}$  for (30, 45, 60 and 75) min under a vacuum of approximately  $1.33 \times 10^{-4}$  mbar in a vacuum furnace.

The bonded specimens were sectioned perpendicular to the bond. The microstructure of the joints was studied using an optical microscope and a scanning electron microscope (SEM). For the microstructural examinations the specimens were etched using two etchants. The Murakami etchant (10 g KOH, 10 g  $\text{K}_3[\text{Fe}(\text{CN})_6]$ , 100 ml  $\text{H}_2\text{O}$ ) preferentially etches the Cr-rich phases and can therefore be used to reveal precipitates adjacent to the joint/base metal interface. The molybdenum-acid etchant (0.5 g  $\text{MoO}_3$ , 50 ml HCl, 50 ml  $\text{HNO}_3$ , 200 ml  $\text{H}_2\text{O}$ ), which preferentially etches the  $\gamma$ '-phase, was used to indicate the  $\gamma$ - $\gamma'$ -microstructure of the joints. Semi-quantitative chemical analyses of the phases formed in the joint region were conducted on a Cam Scan scanning electron microscope, equipped with a beryllium-window energy-dispersive spectrometer (EDS) system using INCA software.

## 3 RESULTS AND DISCUSSION

### 3.1 Microstructure of the bond

The microstructure of the TLP-bonded GTD-111/Ni-Si-B/GTD-111 is detailed elsewhere.<sup>4,6</sup> In this section a summary of the results is presented. **Figure 2a** shows an SEM image of the bonds made at 1100  $^{\circ}\text{C}$  for 30 min, indicating three distinct microstructural zones in the bond region including (i) an isothermal solidification zone (ISZ), (ii) a diffusion-affected zone (DAZ) and (iii) an athermal solidification zone. The formation of these zones can be explained as follows:

Since the bonding temperature (i.e., 1100  $^{\circ}\text{C}$ ) is higher than the liquidus temperature of the Ni-Si-B filler alloy (i.e., 1055  $^{\circ}\text{C}$ ), the interlayer melts. Three transportation phenomena occur during the TLP bonding of the IN718/Ni-4.5Si-3.2B/IN718, including the following:

- Dissolution of the BM,
- Diffusion of MPD elements (Si and B) from the molten interlayer into the BM,
- Diffusion of Cr, Co, Mo, W, Ta, Al and Ti from the BM into the bond region.

All of these phenomena govern the chemical composition of the liquid phase, which in turn dictates the liquidus temperature of the liquid phase. The effect of alloying elements on the liquidus temperature depends on the distribution coefficient ( $k$ ). Two phenomena help to increase the liquidus temperature of the liquid phase including:

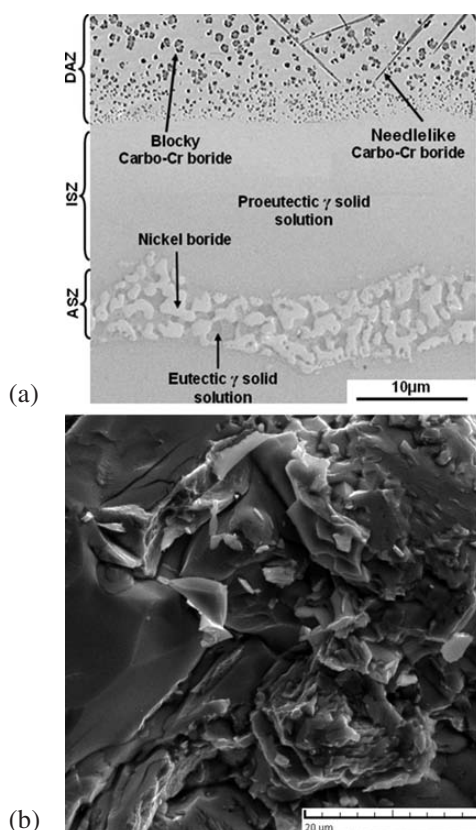


**Figure 2:** a) Microstructure gradient in TLP-bonded GTD-111 using Ni-Si-B filler alloy at 1100  $^{\circ}\text{C}$  for 30 min, b) fracture surface of the TLP bonded sample after partial isothermal solidification

**Slika 2:** a) Spreminjanje mikrostrukture v TLP-spoju GTD-111 z uporabo Ni-Si-B-zlitine polnila 30 min pri 1100  $^{\circ}\text{C}$ , b) površina preloma s TLP spojenega vzorca po delnem izotermnem strjevanju

- Depletion of the liquid phase from the MPD elements that have a  $k$  value less than unity significantly increases the liquidus temperature of the liquid phase.
- Co and W content of the liquid is increased gradually as a result of the BM dissolution phenomenon and the diffusion of Co and W from the BM into the bond region during the bonding process. The presence of Co and W, which exhibit a  $k$  value larger than unity,<sup>16</sup> increase the liquidus temperature.

As a consequence of both phenomena, the liquidus temperature of the liquid phase increases gradually during holding at the bonding temperature. Once the liquidus temperature increased to the bonding temperature, isothermal solidification starts. As a result of the absence of any solute rejection at the solid/liquid interface during isothermal solidification, the formation of the second phase is prevented. The microstructure of this zone consists of a pro-eutectic nickel-rich  $\gamma$  solid-solution phase. The average hardness of this zone was 310 HV.

If the sample is cooled down before completion of the isothermal solidification, the residual liquid would solidify under a different mechanism. The morphology of the product suggests that the structure is formed via a eutectic-type transformation during cooling. During solidification induced by cooling, B is rejected to the liquid in the middle of the joint due to the low solubility of B in the solidifying  $\gamma$  phase. Continuous solute enrichment of the liquid could cause the solute concentration to exceed the solubility limit of the solute in the  $\gamma$  phase. Consequently, any residual liquid could transform into eutectic-type solidification products during cooling from the bonding temperature.<sup>7-10</sup> The microstructure of the ASZ consists of two distinct phases: a nickel-rich solid-solution phase and an intermetallic phase. The average hardness of this zone was 570 HV. The EDS analysis showed<sup>6</sup> that the intermetallic phase is a nickel-rich boride. The solidification sequence can be summarized as follows:



The diffusion-affected zone (DAZ) consists of second-phase particles with two different morphologies: particles with a blocky morphology and particles with a needle-like morphology. Boron and carbon were detected in both types of precipitates using an EDS analysis. The EDS compositional analysis of the metallic elements showed that both precipitates are Cr-rich carbo-boride.<sup>4</sup> The diffusion of boron from the liquid phase into the base metal, coupled with the fact that boron can reduce the solubility of carbon in an austenitic matrix, and the presence of Cr (which is a strong boride former) can explain the formation of Cr-rich carbo-borides.

It is of interest to note that due to the spatially non-continuous distribution along the joint/base-metal interface and the lower hardness compared to that of the eutectic microconstituents, the Cr-rich boride precipita-

tes in the DAZ have a less detrimental effect on the joint strength compared to the ASZ. However, the intermetallic-containing solidification products can serve as the preferential failure source for the brazed joint due to the inherently high hardness and brittleness of the intermetallic phases. Consequently, they can significantly reduce the mechanical properties and creep strength of the joint, especially when the intermetallics are spatially continuous.<sup>8-10</sup> The shear strength of this bond was 310 MPa, which is about 40 % of that of the base metal (780 MPa). A fracture-surface examination showed that the crack propagated along the joint centerline. **Figure 2b** shows a fracture surface of these bonds, indicating a semi-cleavage/intergranular fracture. Therefore, in a situation where isothermal solidification has not been accomplished completely, eutectic micro-constituents that usually have the highest hardness in the bond region and form an interlinked network are the preferential failure source. Therefore, it is necessary to eliminate the eutectic products in order to improve the strength of the joints. The experimental results showed that for a bonding time of 75 min at 1100 °C, in which the eutectic products are completely removed, bonds with a shear strength of 530 MPa (i.e., a joint efficiency of 68 % ) were achieved.

### 3.2 Prediction of the isothermal solidification time

When considering TLP bonding for commercial applications, an important bonding parameter is the holding time required to complete the isothermal solidification ( $t_{IS}$ ). Isothermal solidification is a prerequisite for obtaining a proper bond microstructure during the TLP bonding. If the holding time is lower than  $t_{IS}$ , athermal solidification of the residual liquid phase will lead to intermetallic formation, which in turn degrades the shear strength of the bond. Therefore, in this section, considering the solidification behaviour of residual liquid, a diffusion model based on a migrating interface was used to predict the isothermal solidification's completion time.

Conventional analytical models of TLP bonding are based on binary systems; one of these models is used to estimate  $t_{IS}$  for the GTD-111/Ni-Si-B/GTD-111 multi-components system. Migrating the solid/liquid interface modelling approach was used by several researchers.<sup>17,18</sup> This approach treats the system as two, semi-infinite phases with a coupled diffusion-controlled moving solid/liquid interface (**Figure 3**). Isothermal solidification can be characterized by the motion of the solid-liquid interface, resulting from solid-state diffusion of the melting-point depressant (MPD) into the base metal. Interface motion can be determined by applying conservation of mass at the interface in conjunction with Fick's first law:<sup>18</sup>

$$(C_L - C_S) \frac{dX(t)}{dt} = D_S \frac{\partial C_S}{\partial x} - D_L \frac{dC_L}{dx} \quad (2)$$

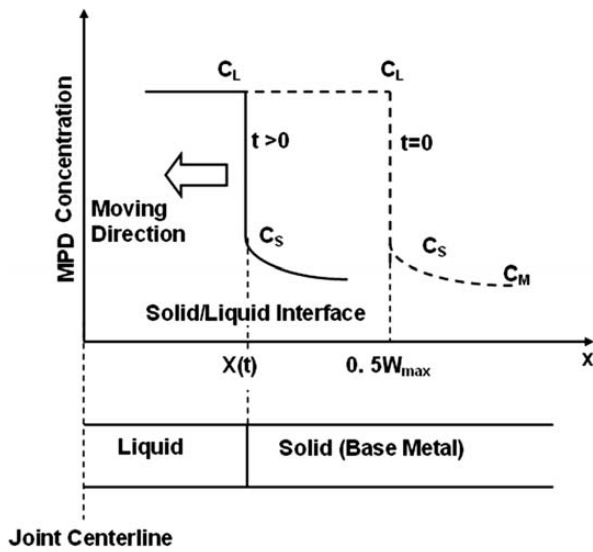


**Figure 3:** Schematic showing solute distribution during isothermal solidification stage during TLP bonding process

**Slika 3:** Shematski prikaz rasporeditve koncentracij med izotermno fazo strjevanja pri TLP-postopku spajanja

Where  $C_L$  and  $C_S$  are the equilibrium liquidus and solidus, respectively, and  $X(t)$  is the liquid/solid interface position. Because of the orders of magnitude difference in the diffusivity of solid and liquid, interface motion is separated into two distinct regimes. During the dissolution stage, the right-hand side of Equation (2) is dominated by the second term containing  $D_{\text{liquid}}$  and the interface moves into the solid until local equilibrium is achieved at the liquid/solid interface. At this point the dissolution ceases. Once the gradient in the liquid reaches zero, the liquid term becomes negligible and the interface begins to move back into the liquid and the isothermal solidification starts. In this condition the kinetics of the TLP process is dominated by Equation (3).<sup>17,18</sup>

$$(C_L - C_S) \frac{dX(t)}{dt} = D \left( \frac{\partial C(x,t)}{\partial t} \right)_{x=X(t)} \quad (3)$$

The concentration profile of the MPD element in the solid can be calculated by applying Fick's second law in the solid and can be satisfied by a general error function solution:

$$C(x,t) = A + B \operatorname{erf} \left( \frac{x}{\sqrt{4Dt}} \right) \quad (4)$$

where  $A$  and  $B$  are constants determined by the following boundary conditions:

$$C(\infty, t) = A + B = C_M \quad (5)$$

$$C(X(t), t) = A + B \operatorname{erf} \left( \frac{x}{\sqrt{4Dt}} \right) = C_S \quad (6)$$

where  $C_M$  is the MPD concentration of the base metal. Since Equation (6) has to be satisfied for all values of  $t$ ,  $X(t)$  must be proportional to  $t^{1/2}$ , hence:

$$X(t) = K \sqrt{4Dt} \quad (7)$$

Equation (7) suggests a linear relationship between the eutectic structure width (ASZ size) and the square root of the bonding time.

At the end of the isothermal solidification, two solid/liquid interfaces meet at the centerline (i.e.,  $X(t)$  reaches half of the maximum liquid width ( $W_{\text{max}}$ )). Therefore, the completion time for isothermal solidification during TLP bonding can be calculated using the following equation:

$$t_{\text{IS}} = \frac{W_{\text{max}}^2}{16K^2D} \quad (8)$$

where the constant  $K$  will be determined by mass conservation at the moving interface. The derivatives of the concentration profile and the interface position can then be substituted into Equation (3) to solve for  $K$ :

$$(C_L - C_S) K \sqrt{\frac{D}{t}} = D_S \frac{C_S - C_M}{1 + \operatorname{erf}(K)} \cdot \frac{2}{\sqrt{4\pi DT}} \exp(-K^2) \quad (9)$$

Rearrangement of Equation (9) leads to:

$$\frac{C_L - C_M}{C_L - C_S} = K \sqrt{\pi} \exp(K^2) (1 + \operatorname{erf} K) \quad (10)$$

Since the calculation of  $K$  needs numerical solving, a linear approximation of the right-hand side of Equation (9), when  $K < 0.1$ , was obtained by MATLAB software:

$$\frac{C_L - C_M}{C_L - C_S} = 2K \quad (11)$$

A combination of Equation (7) and Equation (10) leads to:

$$t_{\text{IS}} = \frac{W_{\text{max}}^2}{4D} \left( \frac{C_L - C_S}{C_S - C_M} \right)^2 \quad (12)$$

The theoretical maximum width of the liquid can be obtained by a simple mass conservation:<sup>18</sup>

$$W_{\text{max}} C_L = W_0 C_{\text{FM}} \quad (13)$$

where  $C_M$  is the MPD concentration of the filler metal.

### 3.3 Model validation

In this section the described model is used to estimate  $t_{\text{IS}}$  for the investigated system. For GTD-111/Ni-Si-B/GTD-111, however, the involved materials are quite complex and there is a lack of detailed diffusion and phase-diagram data. In order to apply the migrating solid/liquid interface and compare it with the experimental results for GTD-111/Ni-Si-B/GTD-111, the following assumptions were taken into consideration:

1. Since Ni is the main element in GTD-111 nickel-based superalloy, the base metal was considered as pure nickel.
2. The solidification behaviour of the ternary Ni-Si-B interlayer could be considered similar to the solidi-

fication behaviour of the binary Ni-B interlayer. Two reasons for this assumption are:

- For multi-component TLP systems, the kinetics of the solid/liquid interface movement is controlled by a faster solute,<sup>19</sup> which is boron in the case of the GTD-111/Ni-Si-B/GTD-111 system. The diffusion coefficient of boron in nickel is about  $10^4$  times greater than that of the silicon in the nickel substrate.
- As mentioned above, the eutectic type structure resulting from non-equilibrium solidification of the residual liquid consists of a  $\gamma$ -solid solution and nickel boride, and no silicide was observed in the ASZ microstructure. Indeed, the low solubility of boron in the nickel-based substrates resulted in the formation of intermetallic phases in the eutectic structure of the ASZ.

The thermodynamic data that were used for prediction of  $t_{IS}$ , are:

$$x(C_S) = 0.3 \% \text{ B (based on Ni-B binary phase diagram}^{20})$$

$$x(C_L) = 13.16 \% \text{ B (based on liquidus composition for Ni-Si-B filler}^{21})$$

$$x(C_M) = 0$$

$$x(C_{FM}) = 13.6 \% \text{ B (based on the initial composition of interlayer) (mole fractions } x)$$

The diffusion coefficient of boron in GTD-111 will be needed to calculate the  $t_{IS}$ . Unfortunately, there is little data for the diffusion coefficient of boron in nickel-based superalloys. The diffusion coefficient of boron out of a Ni-Cr-Si-B filler metal in a nickel-based substrate at a temperature of 1100 °C was determined by Kukera et al.<sup>22</sup> to be  $6.22 \times 10^{-11} \text{ m}^2/\text{s}$ .

**Figure 4** shows a plot of ASZ size (or eutectic width) vs. square root of the bonding time. The eutectic width decreases linearly with the square root of bonding time. Therefore, the migrating interface model is applicable for the system that is used in this study. Also, solving equation (9) numerically with these data yields 12.96

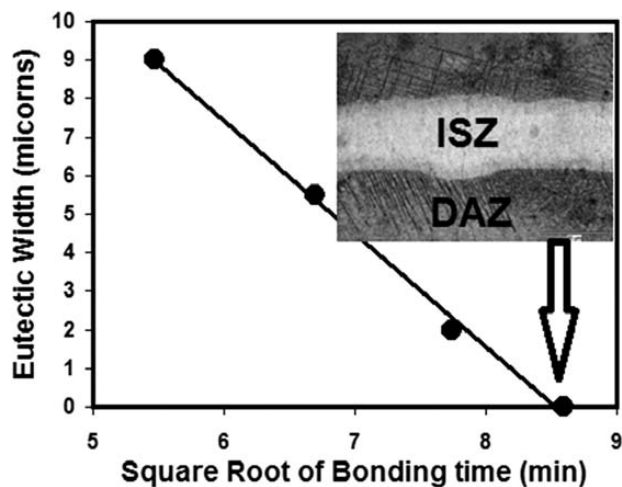


**Figure 4:** The width of eutectic-type micro-constituents versus square root of bonding time for TLP bonding of GTD-111/Ni-Si-B/GTD-111

**Slika 4:** Širina evtetičnih faz v odvisnosti od kvadrata časa spajanja za TLP-spajanje GTD-111/Ni-Si-B/GTD-111

$\times 10^{-3}$  for  $K$ , which is considerably less than 0.1, supporting the applicability of Equation (12) in the present work.

According to the above data and using Equation (12) the resulting value for  $t_{IS}$  is 89 min. Experimental results showed that at bonding temperatures of 1100 °C, bonds free from the centerline eutectic were obtained after 75 min. **Figure 5** shows the typical microstructure of the bonds made at 1100 °C for 75 min, indicating a eutectic-free joint. The absence of a eutectic-type structure in the joint centerline suggests the completion of isothermal solidification under this bonding condition. As can be seen, this model can predict  $t_{IS}$  with a reasonable accuracy. A good agreement between the time calculated for  $t_{IS}$  (89 min) and that experimentally observed (75 min) was obtained. This difference can be attributed to the liquid penetration into the grain boundaries of the base metal, grain-boundary migration, loss of liquid metal by the squeezing-out action<sup>23,24</sup> and the simplified assumptions of the model. It should be noted that the accuracy of the  $t_{IS}$  prediction is largely dependent on the diffusion data. Despite some discrepancy between the experimental and predicted values, this modelling can be considered as the first step for the designing and optimization of process parameters to achieve an appropriate TLP bond microstructure.

Finally, it is interesting to note that isothermal solidification completion prevents the formation of a eutectic structure in the bond region; however, significant amounts of Cr-rich carbo-boride were still present in the DAZ (**Figure 5**). The high Cr content of these precipitates leads to a significant depletion of Cr around this region. Because of the fact that Cr is the key element for the corrosion resistance of the superalloy,<sup>25</sup> its depletion can reduce the local corrosion resistance of the matrix.<sup>26–28</sup> It has been reported previously that the corrosion resistance of a brazed superalloy was impaired by the precipitation of Cr-rich particles within the braze/base-alloy interface.<sup>29</sup> Therefore, in order to restore the corrosion resistance of the substrate, it is necessary to design a proper post-bond heat treatment (PBHT) to eliminate the boride precipitates in the DAZ via a break-up and dissolution processes.

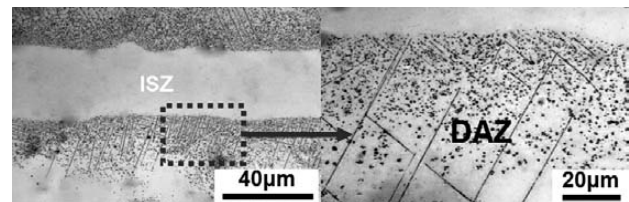


**Figure 5:** Microstructure of TLP bonded GTD-111 at 1100 °C for 75 min showing eutectic-free joint centerline. Extensive boride precipitates are present in the diffusion-affected zone (DAZ).

**Slika 5:** Mikrostruktura TLP-spoja GTD-111 po 75 min na 1100 °C prikazuje srednjo linijo brez evtetika. Številni izločki borida so prisotni v difuzijsko vplivanem področju (DAZ).

## 4 CONCLUSIONS

The isothermal solidification process during the TLP bonding of the GTD-111 nickel-based superalloy using an amorphous Ni-Si-B interlayer was studied. The following conclusions can be drawn from this study:

1. When the bonding time is not sufficient to complete the isothermal solidification (i.e., a bonding time of less than 75 min at bonding temperatures of 1100 °C), the residual liquid phase after an incomplete isothermal solidification at the bonding temperature was transformed to a eutectic type structure consisting of the  $\gamma$ -solid-solution phase and the boride intermetallic. According to the solidification behaviour and the ASZ microstructure, boron is main controlling MPD element of the isothermal solidification.
2. It was found that there is a linear relationship between the eutectic width and the square root of the bonding time, suggesting that the isothermal solidification process is governed by solid-state diffusion.
3. The time required for the completion of isothermal solidification during the TLP bonding of the GTD-111 superalloy could be predicted with fairly good accuracy using a mathematical solution of the time-dependent diffusion equation based on Fick's second law.

## 5 REFERENCES

- <sup>1</sup> A. Milosavljevic, S. Petronic, S. Polic-Radovanovic, J. Babic, D. Bajic, The influence of the heat treatment regim on a fracture surface of nickel-based superalloys, *Mater. Tehnol.*, 46 (2012) 4, 411–417
- <sup>2</sup> R. Sunulahpašić, M. Oruč, M. Hadžalić, M. Rimac, Optimization of the mechanical properties of the superalloy Nimonic 80A, *Mater. Tehnol.*, 46 (2012) 3, 263–267
- <sup>3</sup> A. Semenov, S. Semenov, A. Nazarenko, L. Getsov, Computer simulation of fatigue, creep and thermal-fatigue cracks propagation in gas-turbin blades, *Mater. Tehnol.*, 46 (2012) 3, 197–203
- <sup>4</sup> M. Pouranvari, A. Ekrami, A. H. Kokabi, Microstructure development during transient liquid phase bonding of GTD-111 nickel-based superalloy, *J Alloys Comp*, 461 (2008), 641–647
- <sup>5</sup> M. Pouranvari, A. Ekrami, A. H. Kokabi, TLP bonding of cast IN718 nickel based superalloy: Process–microstructure–strength characteristics, *Mater. Sci. Eng. A*, 568 (2013), 76–82
- <sup>6</sup> M. Pouranvari, A. Ekrami, A. H. Kokabi, Microstructure-properties relationship of TLP-bonded GTD-111 nickel-base superalloy, *Mater. Sci. Eng. A*, 490 (2008), 229–234
- <sup>7</sup> D. S. Duvall, W. A. Owczarski, D. F. Paulonis, TLP Bonding: A new method for joining jeat resistant alloys, *Weld. J.*, 53 (1974), 203–214
- <sup>8</sup> O. A. Ojo, N. L. Richards, M. C. Chaturvedi, Effect of gap size and process parameters on diffusion brazing of Inconel 738, *Sci. Technol. Weld. Joining*, 9 (2004), 209–220
- <sup>9</sup> M. Pouranvari, A. Ekrami, A. H. Kokabi, Effect of bonding temperature on microstructure development during TLP bonding of a nickel base superalloy, *J Alloys Comp.*, 469 (2009), 270–275
- <sup>10</sup> W. F. Gale, D. A. Butts, Transient liquid phase bonding, *Sci. Technol. Weld. Joining*, 9 (2004), 283–300
- <sup>11</sup> F. Jalilian, M. Jahazi, R. A. L. Drew, Microstructural evolution during transient liquid phase bonding of Inconel 617 using Ni-Si-B filler metal, *Mater. Sci. Eng. A*, 447 (2007), 125–33
- <sup>12</sup> M. Pouranvari, A. Ekrami, A. H. Kokabi, Effect of the Bonding Time on the Microstructure and Mechanical Properties of a Transient Liquid Phase Bonded IN718 using a Ni-Cr-B Filler Alloy, *Mater. Tehnol.*, 47 (2013) 5, 593–599
- <sup>13</sup> N. R. Philips, Microstructural Evolution and Ductile Phase Toughening in Brazed Joints, Phd Thesis, University of California, 2008
- <sup>14</sup> I. Tuah-Poku, M. Dollar, T. B. Massalski, A study of the transient liquid phase bonding process applied to a Ag/Cu/Ag sandwich joint, *Metall. Trans. A*, 9 (1988), 675–686
- <sup>15</sup> G. Humpston, D. M. Jacobson, Principles of soldering and brazing, ASM International, Metals Park, Ohio 1993
- <sup>16</sup> O. A. Ojo, N. L. Richards, M. C. Chaturvedi, Microstructural study of weld fusion zone of TIG welded IN 738LC nickel-based superalloy, *Scripta Materialia*, 51 (2004), 683–688
- <sup>17</sup> O. A. Ojo, N. L. Richards, M. C. Chaturvedi, Isothermal solidification during transient liquid phase bonding of Inconel 738 superalloy, *Sci. Technol. Weld. Joining*, 9 (2004), 532–540
- <sup>18</sup> Y. Zhou, W. F. Gale, T. H. North, Modelling of transient liquid phase bonding, *Int. Mater. Rev.*, 40 (1995), 181–196
- <sup>19</sup> C. W. Sinclair, G. R. Purdy, J. E. Morral, Transient liquid-phase bonding in two-phase ternary systems, *Metall. Trans. A.*, 31A (2000), 1187–1192
- <sup>20</sup> T. B. Massalski (ed.), Binary alloy phase diagrams, ASM International, Metals Park, OH 1986, 366–371
- <sup>21</sup> S. Omori, Y. Hashimoto, K. Shoji, K. Hidaka, Y. Kohira, *Jpn Soc. Powder metal.*, 18 (1972), 316–320
- <sup>22</sup> J. Kukera, A. Buchal, A. Rek, K. Stransky, *Kovove Mater.*, 22 (1984), 250–262
- <sup>23</sup> T. Padron, T. I. Khan, M. J. Kabir, Modelling the transient liquid phase bonding behaviour of a duplex stainless steel using copper interlayers, *Mater. Sci. Eng. A*, 385 (2004), 220–228
- <sup>24</sup> W. D. MacDonald, T. W. Eagar, Isothermal solidification kinetics of diffusion brazing, *Metall. Matter. Trans A*, 29 (1998), 315–32
- <sup>25</sup> J. Lippold, S. D. Kiser, J. N. DuPont, *Welding Metallurgy and Weldability of Nickel-Base Alloys*, Wiley publishing, 2009
- <sup>26</sup> M. Pouranvari, A. Ekrami, A. H. Ekrami, Solidification and Solid State Phenomena during TLP bonding of IN718 Superalloy Using Ni-Si-B Ternary Filler Alloy, *J Alloys Comp*, 563 (2013), 143–149
- <sup>27</sup> M. Pouranvari, A. Ekrami, A. H. Kokabi, Transient Liquid Phase Bonding of Wrought IN718 Nickel Based Superalloy Using Standard Heat Treatment Cycles: Microstructure and Mechanical Properties, *Materials & Design*, 50 (2013), 694–701
- <sup>28</sup> O. A. Idowu, O. A. Ojo, M. C. Chaturvedi, Microstructural Study of Transient Liquid Phase Bonded Cast INCONEL 738LC Superalloy, *Metall Mater Trans A*, 37A (2006), 2787–2796
- <sup>29</sup> B. Jahnke, J. Demny, Microstructural investigations of a nickel-based repair coating processed by liquid phase diffusion sintering, *Thin Solid Films*, 110 (1983), 225–35